# FIRE RESISTANCE OF AXIALLY LOADED SLENDER CONCRETE FILLED STEEL TUBULAR COLUMNS. Development of a three-dimensional numerical model and comparison with Eurocode 4.

Ana Espinós, Antonio Hospitaler, Carmen Ibáñez, Manuel L. Romero
Instituto de Ciencia y Tecnología del Hormigón (ICITECH)
Universidad Politécnica de Valencia

## NUMERICAL MODEL

- Non-linear FE analysis package ABAQUS
- Parts: concrete core + steel tube ⇒ ASSEMBLY
- Eight-node three-dimensional solid elements (C3D8RT)
- Additional variable: Nodal temperature (NT11)
- Element size < 2 cm

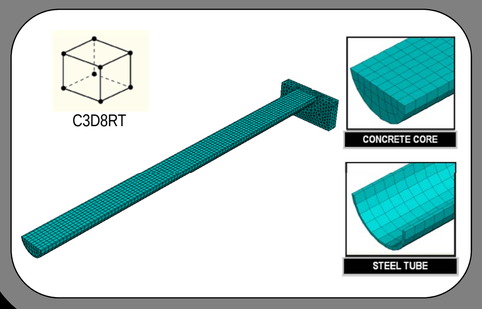


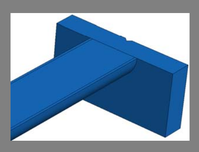

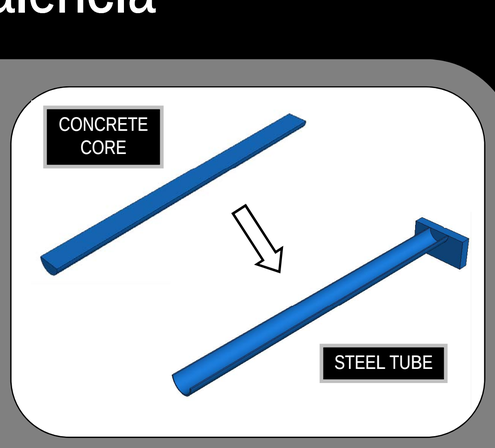


PARAMETERS
- Length of the column (*L*)
- External diameter (*D*)
- Thickness of the steel tube (*t*)
- Axial load level ($\mu = N / N_{pl}$)
- Concrete resistance ($f_{ck}$) and steel resistance ($f_y$)

## MATERIAL PROPERTIES AT ELEVATED TEMPERATURES

CONCRETE
- Thermal properties according to EC2 Part 1-2
- $\alpha_c$ = 6 x $10^{-6}$ $^oC^{-1}$ (Hong-Varma, 2009)
- Stress-strain curves proposed by prof. Lie (1994)

$$\varepsilon_c = \varepsilon_{th}(\theta_c) + \varepsilon_\sigma(\sigma_c,\theta_c) + \varepsilon_{cr}(\sigma_c,\theta_c,t) + \varepsilon_{tr}(\sigma_c,\theta_c)$$

STEEL
- Thermal and mechanical properties according to EC3 Part 1-2
- $\alpha_S$ = 12 x $10^{-6}$ $^oC^{-1}$ (Hong-Varma, 2009)

$$\varepsilon_a = \varepsilon_{th}(\theta_a) + \varepsilon_\sigma(\sigma_a,\theta_a) + \varepsilon_{cr}(\sigma_a,\theta_a,t)$$

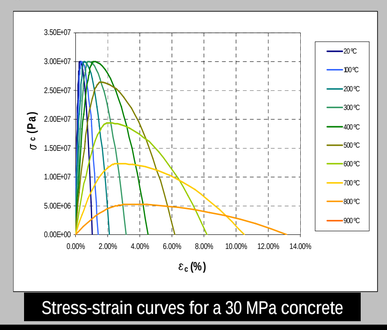


Stress-strain curves for a 30 MPa concrete

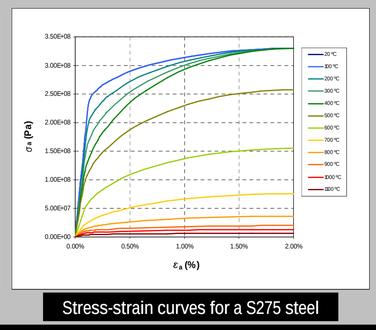


Stress-strain curves for a S275 steel

STRAIN COMPONENTS
- $\varepsilon_{th}$ ⇒ Free thermal strain
- $\varepsilon_\sigma$ ⇒ Stress-related strain
- $\varepsilon_{cr}$ ⇒ Creep strain
- $\varepsilon_{tr}$ ⇒ Transient strain

## STEEL-CONCRETE INTERFACE. MECHANICAL CONTACT

**Normal behaviour**

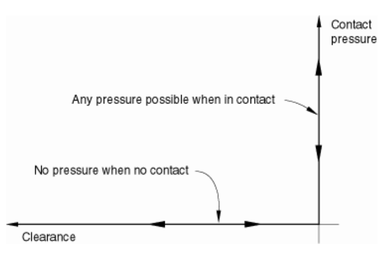


"Hard" contact (pressure-overclosure relationship)

**Frictional behaviour**

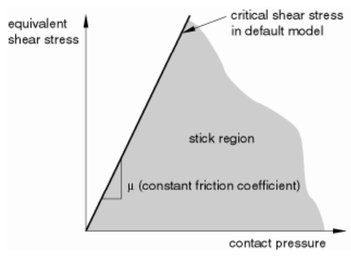


Coulomb friction model (slip regions)

## STEEL-CONCRETE INTERFACE. THERMAL CONTACT

- Gap conductance: $q = k(\theta_A - \theta_B)$
  - $k$ ⇒ Gap conductance
  - $\theta_A$ ⇒ Temperature of point A (slave surface)
  - $\theta_B$ ⇒ Temperature of point B (master surface)

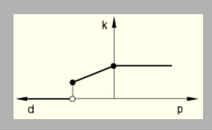


Gap conductance as a function of clearance

- Gap radiation: $q = C\left((\theta_A - \theta^Z)^4 - (\theta_B - \theta^Z)^4\right)$
  - $\theta^Z$ ⇒ Absolute zero
  - $F$ ⇒ Effective viewfactor
  - $\varepsilon_A$ ⇒ Surface A emissivity
  - $\varepsilon_B$ ⇒ Surface B emissivity

$$C = \frac{F\sigma}{1/\varepsilon_A + 1/\varepsilon_B - 1}$$

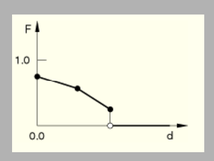


Viewfactor as a function of clearance

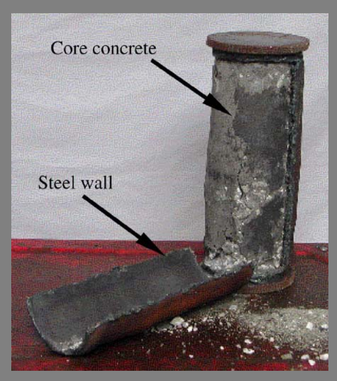


Han LH et al., 2005.

## VALIDATION OF THE MODEL. THERMAL RESPONSE

- ISO-834 standard fire curve

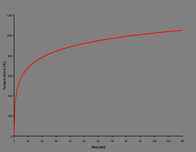

$\alpha_c = 25\ \mathrm{W/m^2K}$
$\Phi = 1$
$\sigma = 5.67 \cdot 10^{-8}\ \mathrm{W/m^2K^4}$
$\varepsilon_m = 0.7$
$\varepsilon_f = 1$

- Comparison with Lie's finite differences model (Lie TT, 1994)

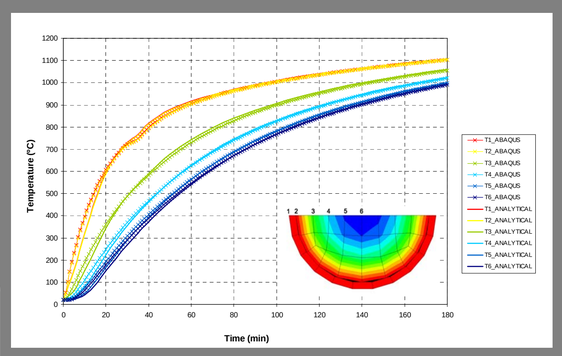


Cross-sectional temperature distribution for a CFT 141x6.5 mm column

Heat transfer equation: $\rho c \dfrac{\partial \theta}{\partial t} = \nabla \cdot (\lambda \nabla \theta) + Q$

Boundary conditions: $\lambda \dfrac{\partial \theta_m}{\partial n} = \dot{h}_{net}$ $\quad \dot{h}_{net} = \dot{h}_{net,c} + \dot{h}_{net,r}\ (\mathrm{W/m^2})$

- Convection: $\dot{h}_{net,c} = \alpha_c \cdot (\theta_g - \theta_m)\ (\mathrm{W/m^2})$
- Radiation: $\dot{h}_{net,r} = \Phi \cdot \varepsilon_m \cdot \varepsilon_f \cdot \sigma \cdot \left[(\theta_r + 273)^4 - (\theta_m + 273)^4\right]\ (\mathrm{W/m^2})$

## VALIDATION OF THE MODEL. MECHANICAL RESPONSE

- Some of the specimens previously tested by Lie et al. (1988) at the "National Research Council" of Canada were simulated:
  - Circular hollow sections
  - Filled with plain concrete
  - Concentric compression load
  - *L* = 3810 mm ($L_{exposed}$ = 3048 mm)
  - Fix-ended

| Column specimen | D (mm) | t (mm) | $f_y$ (N/mm$^2$) | $f_{ck}$ (N/mm$^2$) | N (kN) | $\mu = N / N_{pl,Rd}$ | FRR (min) |
|---|---|---|---|---|---|---|---|
| 1 | 141 | 6.5 | 401.93 | 28.62 | 131 | 8.90% | 57 |
| 2 | 168 | 4.8 | 346.98 | 28.62 | 218 | 15.37% | 56 |
| 3 | 219 | 4.8 | 322.06 | 24.34 | 492 | 26.19% | 80 |
| 4 | 219 | 4.8 | 322.06 | 24.34 | 384 | 20.44% | 102 |
| 5 | 219 | 8.2 | 367.43 | 24.34 | 525 | 18.88% | 82 |
| 6 | 273 | 5.6 | 412.79 | 26.34 | 574 | 17.08% | 112 |
| 7 | 273 | 5.6 | 412.79 | 26.34 | 525 | 15.63% | 133 |
| 8 | 273 | 5.6 | 412.79 | 26.34 | 1000 | 29.76% | 70 |

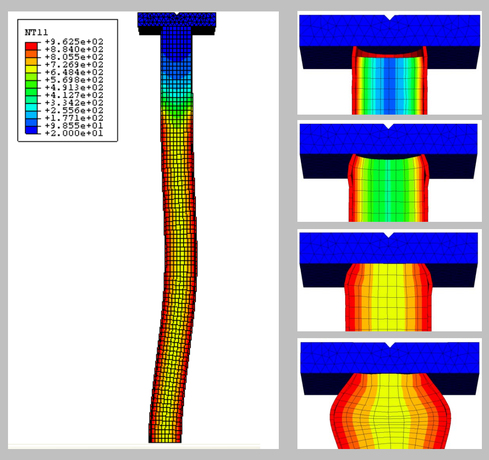


## RESULTS

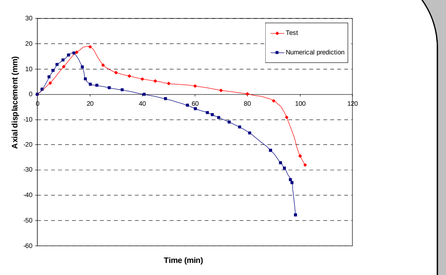


Comparison between calculated and measured axial displacement, for tests no. 4 and 7

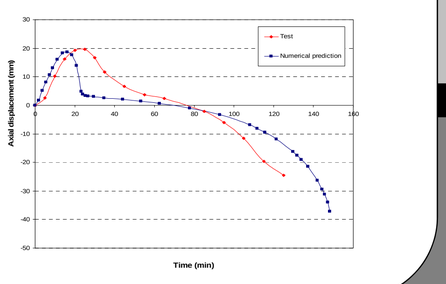


| Column specimen | FRR (min) Test | FRR (min) Simulation | $\xi_{FRR} = \frac{FRR_{test}}{FRR_{NS}}$ | $\delta_{max}$ (mm) Test | $\delta_{max}$ (mm) Simulation | $\xi\ \delta_{max} = \frac{\delta_{max,test}}{\delta_{max,NS}}$ |
|---|---|---|---|---|---|---|
| 1 | 57 | 72 | 0.79 | 24.09 | 24.35 | 0.99 |
| 2 | 56 | 75 | 0.75 | 20.48 | 19.25 | 1.06 |
| 3 | 80 | 74 | 1.08 | 18.13 | 12.36 | 1.47 |
| 4 | 102 | 97 | 1.05 | 18.77 | 16.23 | 1.16 |
| 5 | 82 | 68 | 1.21 | 20.36 | 19.30 | 1.05 |
| 6 | 112 | 126 | 0.89 | 16.40 | 17.71 | 0.93 |
| 7 | 133 | 137 | 0.97 | 19.67 | 18.61 | 1.06 |
| 8 | 70 | 70 | 1.00 | 5.51 | 10.35 | 0.53 |
| | | Average | **0.97** | | Average | **1.03** |
| | | Standard deviation | **0.15** | | Standard deviation | **0.26** |

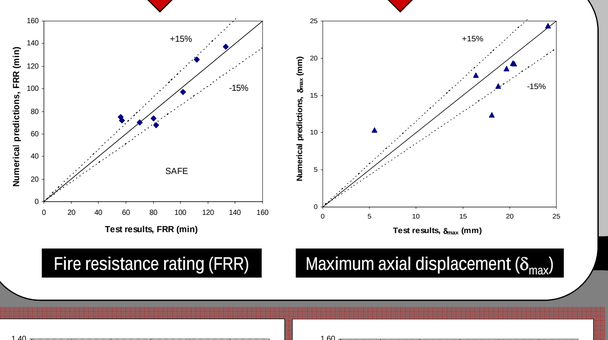


Fire resistance rating (FRR) | Maximum axial displacement ($\delta_{max}$)

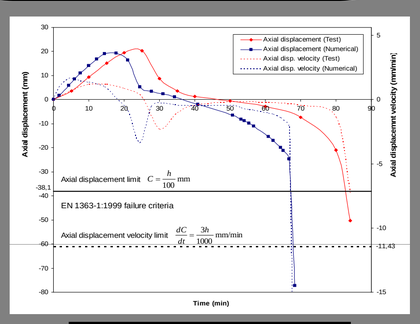


Determination of the FRR (test no. 5)

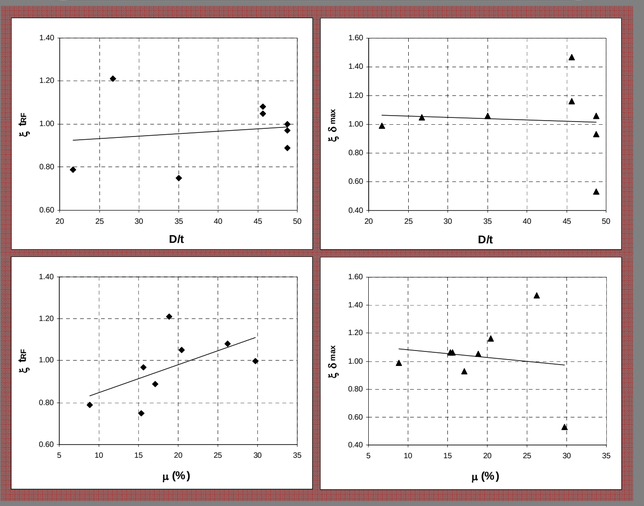


## COMPARISON WITH EC4 SIMPLIFIED CALCULATION MODEL

- The proposed numerical model gives a better prediction of the fire resistance rating, showing a very accurate trend.
- The EC4 simplified model doesn't take into account the thermal expansion of the materials, nor the air gap at the steel-concrete boundary, what lies on the safe side and gives a very conservative prediction.
- If we apply these simplifications to our numerical model, smaller values of the fire resistance ratings are obtained, very similar to those predicted by EC4.

| Column specimen | FRR (min) Test | Simulation | Simulation (no expansion) | EC4 | $\xi_{FRR} = \frac{FRR_{test}}{FRR_{calc}}$ Simulation | Simulation (no expansion) | EC4 |
|---|---|---|---|---|---|---|---|
| 1 | 57 | 72 | 49 | 49 | 0.79 | 1.16 | 1.16 |
| 2 | 56 | 75 | 46 | 46 | 0.75 | 1.22 | 1.22 |
| 3 | 80 | 74 | 52 | 49 | 1.08 | 1.54 | 1.63 |
| 4 | 102 | 97 | 63 | 61 | 1.05 | 1.62 | 1.67 |
| 5 | 82 | 68 | 52 | 51 | 1.21 | 1.58 | 1.61 |
| 6 | 112 | 126 | 118 | 91 | 0.89 | 0.95 | 1.23 |
| 7 | 133 | 137 | 126 | 96 | 0.97 | 1.06 | 1.39 |
| 8 | 70 | 70 | 58 | 56 | 1.00 | 1.21 | 1.25 |
| | | | | Average | **0.97** | **1.29** | **1.39** |
| | | | | Standard deviation | **0.15** | **0.25** | **0.21** |

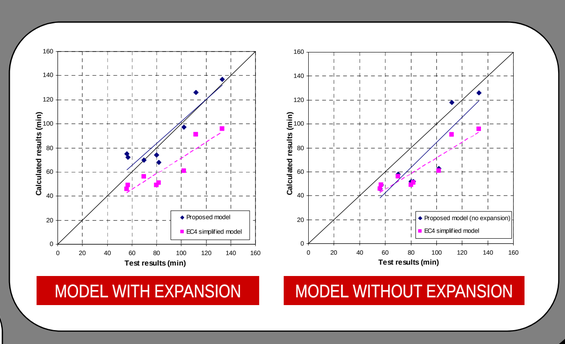


MODEL WITH EXPANSION | MODEL WITHOUT EXPANSION

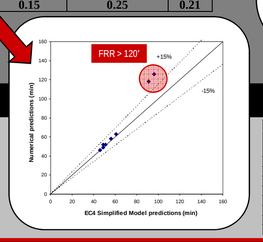


| Column specimen | $\xi_{FRR} = \frac{FRR_{EC4}}{FRR_{NS}}$ |
|---|---|
| 1 | 1.00 |
| 2 | 1.00 |
| 3 | 0.94 |
| 4 | 0.97 |
| 5 | 0.98 |
| 6 | 0.77 |
| 7 | 0.76 |
| 8 | 0.97 |

## CONCLUSIONS

It is possible to reproduce the EC4 simplified calculation model predictions by assuming full thermal contact in the steel-concrete interface and removing the thermal expansion of the materials, what lies on the safe side.

In order to simulate the real behaviour of the column under fire, the thermal expansion of steel and concrete must be taken into account, what extends the failure time.

The proposed numerical model provides more accurate predictions than the EC4 simplified calculation model, which tends to be excesively conservative in most cases.

The thermal expansion of the steel tube produces an opposed axial strain in the early stages of heating, as well as an opening of the gap in the steel-concrete interface, which delays the heating of the concrete core and thus increases the fire resistance rating.